Dalton Transactions

Dinuclear CoIIYIII vs Tetranuclear Co2IIY2III complexes: The effect of increasing molecular size on magnetic anisotropy and relaxation dynamics

Journal:	*Dalton Transactions*
Manuscript ID	DT-ART-07-2019-002969.R3
Article Type:	Paper
Date Submitted by the Author:	04-Sep-2019
Complete List of Authors:	Masegosa, Alberto; Universidad de Granada Palacios, Maria A.; Universidad de Granada, Inorganic Chemistry Ruiz, Eliseo; Universitat de Barcelona, Departamento de Quimica Inorganica Gómez-Coca, Silvia; Universitat de Barcelona, Departament de Química Inorgànica Krzystek, Jurek; National High Magnetic Field Laboratory, Condensed Matter Science Moreno, Jose M.; Universidad de Granada Colacio, Enrique; Universidad de Granada, Inorganic Chemistry

Dinuclear $Co^{II}Y^{III}$ vs Tetranuclear $Co_2^{II}Y_2^{III}$ complexes: The effect of increasing molecular size on magnetic anisotropy and relaxation dynamics.

Alberto Masegosa,[⊥] María A. Palacios,[⊥] Eliseo Ruiz[#,*], Silvia Gómez-Coca,[#] J. Krzystek,[¶,*] José. M. Moreno,[⊥] Enrique Colacio[⊥,*]

[⊥]Departamento de Química Inorgánica, Facultad de Ciencias, Universidad de Granada, 18071 Granada, Spain

[#]Departament de Química Inorgànica and Institut de Recerca de Química Teòrica i Computacional, Universitat de Barcelona, Diagonal 645, Barcelona E-08028, Spain

[¶] National High Magnetic Field Laboratory, Florida State University, Tallahassee, Florida 32310, USA

Abstract

A new $Co^{II}_2Y^{III}_2$ complex with the formula $[\{Co(\mu\text{-}L)Y(NO_3)\}_2(\mu\text{-}CO_3)_2]\cdot 2CH_3OH\cdot 2H_2O$ (where H_2L = N,N',N''-trimethyl-N,N''-bis(2-hydroxy-3-methoxy-5-methylbenzyl) diethylenetriamine) has been prepared and its structure solved by single-crystal X-Ray diffraction. The tetranuclear structure is formed by the connection of two $[Co(\mu\text{-}L)Y(NO_3)]$ dinuclear units through two carbonate bridging ligands, which exhibit a μ_3–κ^2–O,O : κ-O : κ-O'' tetradentate coordination mode. The Co^{II} ion exhibits a slightly distorted octahedral CoN_3O_3 coordination environment. From direct-current magnetic data a large and positive axial anisotropy parameter was extracted (D = +82.62 cm^{-1}) and its sign unambiguously confirmed by HFEPR spectra and *ab initio* calculations. The extracted D value is rather larger than those previously reported for the analogous $Co^{II}Y^{III}$ dinuclear complexes, which agrees with the fact that the Co^{II} ion in the $Co^{II}_2Y^{III}_2$ complex exhibits the lower distortion from the octahedral geometry in this family of $Co^{II}_nY^{III}_n$ complexes. Dynamic *ac* magnetic measurements show that the reported compound presents field-induced slow relaxation for magnetization reversal, through a combination of direct and Raman processes. Magnetic measurements on the diluted magnetic counterpart (Zn/Co = 10/1) show the persistence of these processes, pointing out their single-ion origin. The Raman relaxation process for the Co_2Y_2 complex is faster that those observed for the CoY dinuclear counterparts. This fact and the existence of the persistent direct process at low temperature could be because the former molecule is larger and flexible than the latter ones.

Introduction

Single-Molecule Magnets (SMMs) are an appealing type of molecular magnetic materials based on discrete metal complexes, which are attracting the research attention some thirty years ago.[1] The field of SMMs lies at the boundary between the quantum and classical worlds. Thus, they display classical properties, such as slow relaxation of the magnetization, responsible for magnetic hysteresis (similar to that of bulk magnets) below the so-called blocking temperature (T_B), and quantum properties, such quantum tunnelling of magnetization (QTM), quantum phase interference and quantum coherence.[1,2] The fascinating physical properties of these nanomagnets make of SMMs promising candidates for potential future applications, among other areas, in ultra-high density magnetic information storage, nanotechnology, molecular spintronics, and as qubits for quantum computing at molecular level.[2] The SMM behaviour arises from the existence of an energy barrier (U) for the magnetization reversal within the bistable magnetic ground state. This energy barrier permits blocking of the molecular magnetization either parallel or antiparallel to the magnetic field when the polarizing field is removed below T_B, thus leading to slow relaxation of the magnetization . The earlier examples of SMMs were polynuclear metal complexes containing anisotropic transition and lanthanide metal ions,[3] because magnetic anisotropy is an essential requirement for existing U and SMM behaviour.[4] However, owing to the fact that the anisotropy of the whole molecule is difficult to control in polynuclear metal complexes, low values of the molecular magnetic anisotropy are generally observed, particularly in the case of transition metal clusters.[5] In view of this, the research in this field is focused on mononuclear SMMs (also called Single-Ion magnets, SIMs), which can exhibit larger anisotropy than their polynuclear counterparts. This strategy has been shown to be the most appropriate to achieve SMMs with improved properties. Specifically, some Dy^{III} SIMs exhibit T_B as high as 80 K,[6] and one of the high temperature SMM is soluble and stable and therefore good candidate for technological applications.[7]

In SIMs based on transition metal ions, the magnitude of D is dictated by the angular momentum, which in turn is modulated by the type of metal ion (coordination number, oxidation state, nature of the ground spin state). Low coordination numbers and oxidation states promote weak ligand fields, which favour large values of the orbital angular momentum and therefore a strong spin-orbit coupling and magnetic anisotropy.[8] In addition, for integer spin systems, an under-barrier tunnelling mechanism occurs, quenching slow relaxation even in the presence of magnetic field, whereas for non-integer spin systems (Kramers ions), in absence of magnetic field, neither direct phonon-induced nor QTM transitions between the states of the ground doublet can be induced by the modulation of the crystal field (van Vleck cancellation)[9].

Moreover, the lack of fast QTM favours Orbach and Raman thermally activated relaxation processes. In view of the above considerations, the research in this field has focused on mononuclear metal complexes with strong magnetic anisotropy, bearing transition metal ions with significant first order orbital angular momentum.[10] This is presumably the reason why mononuclear complexes containing Co^{II} (S =3/2) with different geometries are by far the most studied SIMs.[10] Although the SIMs behaviour has been observed for Co^{II} complexes with both $D > 0$ and $D < 0$, the former ones are much more numerous (including $Co^{II}Y^{III}$ and mixed valence Co^{II}-Co^{III} complexes). It is worth noting that six-coordinated Co^{II} complexes have been widely studied for SIMs behaviour and the results show that those with $D < 0$ are restricted to a few instances, some of them exhibiting slow magnetization relaxation at zero *dc* field above 2 K. However, it has been recently demonstrated using basic principles that six-coordinated Co^{II} complexes with $D > 0$ (easy-plane anisotropy) can in no case exhibit SIMs behaviour at zero field.[9] Nevertheless, in the presence of an applied magnetic field, the electronuclear spin states arising from hyperfine interactions steadily acquire a non-zero magnetic moment due to the Zeeman interactions, and slow relaxation of the magnetization can appear. Recently, we have shown for dinuclear $Co^{II}Y^{III}$ complexes (considered as mononuclear SMMs as the Y^{III} ion is diamagnetic), that, even in the presence of a dc field, slow magnetization relaxation cannot be observed due to the existence of a persistent fast QTM, which is promoted by intermolecular dipolar interactions.[11] By using magnetically diluted Co^{II} complexes prepared by cocrystalization with an isostructural Zn^{II} compound, the intermolecular dipolar interactions and, consequently, the QTM are at least partially suppressed and, in the presence of magnetic field, "hidden SIM" could emerge. As a continuation of this work with $Co^{II}Y^{III}$ complexes, we are interested in analysing how the increase of in size going from a dinuclear $Co^{II}Y^{III}$ to a tetranuclear $Co_2^{II}Y_2^{III}$ complex influences the dynamic magnetic properties. With this aim in mind, in this paper we report the synthesis, X-ray structure, HFEPR spectra, detailed (dc) and (ac) magnetic properties and *ab initio* theoretical calculations of a carbonate–bridged tetranuclear $Co_2^{II}Y_2^{III}$complex with the molecular formula $[\{Co(\mu\text{-}L)Y(NO_3)\}_2(\mu\text{-}CO_3)_2]\cdot 2CH_3OH\cdot 2H_2O$ **1** (H_2L = N,N′,N″-trimethyl-N,N″-bis(2-hydroxy-3-methoxy-5-methylbenzyl) diethylenetriamine). In addition to the role of the size of the complex, we are also interested in investigating how the changes produced by the carbonate-bridging ligand in the distorted octahedral coordination sphere of the Co^{II} ions influence the magnitude of D.

Results and Discussion

Complex **1** has been prepared as pink prismatic-shaped crystals suitable for X-ray analysis from the reaction of H_2L with $Co(NO_3)_2 \cdot 6H_2O$ and subsequently with $Y(NO_3)_3 \cdot 6H_2O$, triethylamine and Na_2CO_3 in MeOH using a 1:1:1:1:2 molar ratio.

The crystal structure of **1** is given in Figure 1, whereas crystallographic data and selected bond lengths and angles are gathered in tables S1 and S2, respectively. Complex **1** crystallizes in the *P2₁/n* space group and is isostructural to the $Zn_2^{II}Dy_2^{III}$ complex previously reported by some of us.[12] The centrosymmetric tetranuclear scaffolding of **1** is made of two [Co(μ-L)Y(NO_3)] dinuclear units joined by two carbonate bridging ligands, which exhibit a μ_3–κ^2–O,O' : κ–O : κ–O" tetradentate coordination mode. The carbonato ligand is coordinated in a chelate mode to the Y^{3+} ion of a $Co^{II}Y^{III}$ dinuclear entity, whereas the third oxygen atom is bonded to the Co^{2+} ion of a centrosymmetrically related dinuclear unit. Moreover, the Y^{3+} ions are bridged by one of the oxygen atoms of the chelating part of each carbonato ligand in a non-symmetric form, generating a rhomboidal $Y(O)_2Y$ bridging unit. Co^{II} and Y^{III} ions of each [Co(μ-L)Y(NO_3)] dinuclear unit are bridged by two phenoxido groups of the L^{2-} ligand. The Co^{II} ion exhibits a slightly trigonally distorted CoN_3O_3 coordination environment, which is formed by the binding in *fac* positions of three oxygen atoms (one belonging to the carbonato ligand and the other two to the phenoxido bridging groups) and the three amine nitrogen atoms of the ligand. The degree of distortion of the Co^{II} coordination polyhedron with respect to the ideal six-vertex polyhedra was calculated using the continuous shape measure theory and SHAPE software (Table S3).[13]The results indicate that the CoN_3O_3 coordination sphere can be considered as intermediate between trigonal prismatic and octahedral ideal geometries, but very close to this latter with CshM values of 11.801 and 1.444, respectively (the rest of ideal geometries present much higher CshM values). The Co-O and Co-N distances are in the 2.0708(17)-2.1542(17) and 2.182(2)-2.250(2) Å range, respectively.

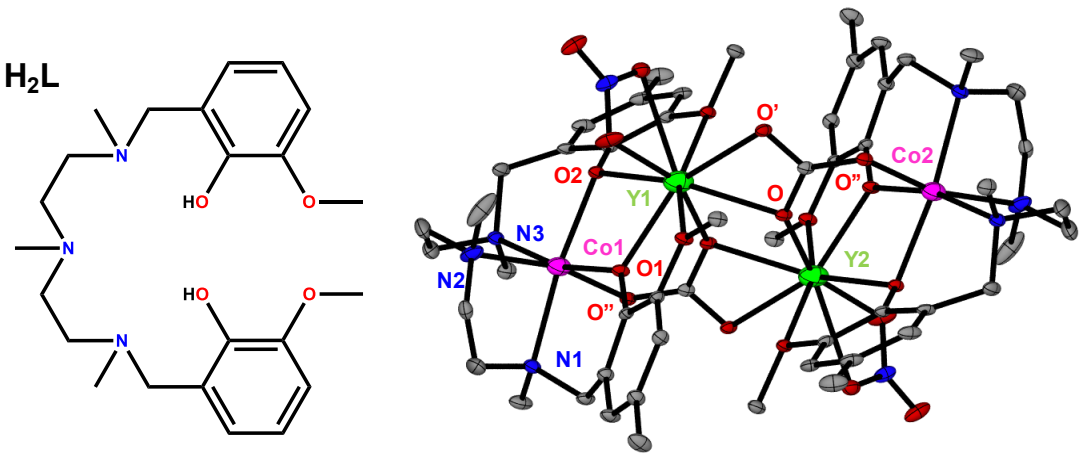

Figure 1. The structure of the ligand H_2L (left) and a perspective view of the structure of **1**. Colour code: N = blue, O = red, Co = pink, Y = green, C = grey. Hydrogen atoms and solvent molecules are omitted for clarity.

The Y^{3+} ion exhibits a somewhat non-symmetrical YO_9 coordination, which is built from the oxygen atoms belonging to the phenoxido bridging groups, the methoxy terminal moieties, the carbonato bridging group and a bidentate nitrate anion. This chelating anion and the chelating part of the carbonato ligand are placed in neighboring positions on the Y^{3+} coordination sphere. The Co···Co, Co···Y and Y···Y distances within the tetranuclear molecule of **1** are 8.278(2), 3.4873(7) and 3.9987(10) Å, respectively. The tetranuclear $\{(\mu_3\text{-}CO_3)_2[Co(\mu\text{-}L)Y(NO_3)]_2\}$ molecules are involved in hydrogen bond interactions with the disordered methanol molecule, so that this latter forms hydrogen bonds with one of the oxygen atoms of the chelating part of the carbonato ligand and with the oxygen atom of a water molecule of a neighboring unit, with donor-acceptor distances of 2.626(5) and 2.718(5) Å and 2.795(7) and 2.744(8) Å, respectively. The shortest internuclear Co^{II}….Co^{II} distances are 8.290(2) and 8.4321(15) Å.

The UV-vis-NIR solid state reflectance spectra of **1** (Figure S1) shows in the visible region a wide band centered at 8400 cm^{-1}, two bands with similar intensity at 19110 cm^{-1} and 20490 cm^{-1} and a shoulder at 18018 cm^{-1}. The first absorption can be assigned to the spin-allowed transition $^4T_{1g}(F) \rightarrow {}^4T_{2g}(F)$, the two bands at intermediate energy are due to the spin allowed $^4T_{1g}(F) \rightarrow {}^4T_{1g}(P)$ transitions split by spin-orbit coupling and the shoulder should correspond to the two electrons spin allowed $^4T_{1g}(F) \rightarrow {}^4A_{2g}(F)$ transition. The values of the octahedral crystal field (10Dq) and the Racah inter-electronic repulsion parameter (B) were calculated from the energy data for the d-d transitions using the appropriate equations[14,15a]. The extracted values 10Dq = 9740 cm^{-1} and B = 849 cm^{-1} are in agreement with those observed for octahedral complexes.[15,16] The nephelauxetic parameter $\beta = B/B_0$ (B_0 = 989 cm^{-1})[17] = 0.86 indicates a significant covalence in the compound. From the Dq and B values, the A parameter, that takes into account the mixture of the ground term $^4T_{1g}(F)$ triplet and the excited term $^4T_{1g}(P)$ was calculated to be A =1.42 (A = 3/2 and 1 for the weak and strong field situations, respectively).[18] This value is consistent with a weak ligand field.

Static dc Magnetic Properties and HFEPR spectroscopy

The temperature dependence of $\chi_M T$, where χ_M is the molar magnetic susceptibility per tetranuclear $Co^{II}_2Y_2^{III}$ unit, was measured for complex **1** in the 2-300 K temperature range under

an applied magnetic field of 0.1 T (Figure 2). The $\chi_M T$ value at room temperature of 6.32 $cm^3mol^{-1}K$ is larger than the calculated spin-only value for two isolated Co^{II} ions with S = 3/2 and g = 2 (3.750 $cm^3mol^{-1}K$), which suggests the existence of unquenched orbital contribution of the Co^{II} ion in a distorted octahedral geometry. On lowering temperature, the $\chi_M T$ product first steadily decreases up to 120 K and then in a sharp manner to reach a value of 4.14 $cm^3mol^{-1}K$ at 2 K. This decrease is essentially due to spin-orbit coupling (SOC) effects.

As the Y^{III} ions are diamagnetic and the $Co^{II}\cdots Co^{II}$ distance is rather long, complex **1** can be considered from the magnetic point of view as two isolated and equivalent mononuclear complexes with distorted octahedral CoN_3O_3 coordination spheres. As indicated above, the continuous shape measures show that the Co^{II} coordination sphere is found in the OC-6 ↔ TPR-6 deformation pathway (with a deviation from this pathway less than 10%). Moreover, it is close to the octahedral geometry, because the square root sum of the S(Oh) and S(TRP) of 4.63 is higher than 4.42, the value for the intermediate geometry.[19] Therefore, the CoN_3O_3 coordination sphere in this compound can be termed as distorted octahedral. The fact that the square root sum of the S(Oh) and S(TRP) is larger than 4.6 suggests the coexistence of a distortion other than the Bailar twist.[19] In the Oh description, the sum of the Co-O2 and Co-N3 bond distances along the O2-Co-N3 axis is about 0.13 Å larger than the corresponding sums along the other two O-Co-N axes. Therefore, the geometry of the CoN_3O_3 coordination sphere could be described as distorted elongated octahedral along the O2-Co-N3 axis. Moreover, this axis presents an axial bending with an O2-Co-N3 angle of 167.31°, as well as slight compressed trigonal and rectangular distortions, this latter in the equatorial CoN1N2O1O2 plane. It has been recently demonstrated,[16] using the angular overlap model, that the combination of these distortions of six-coordinated octahedral complexes are consistent with $\Delta < 0$ (Δ is the axial splitting parameter, see below).

In view of the axial distortion of the coordination sphere of **1**, its magnetic susceptibility data were first analyzed with a model that takes into account: (i) first order SOC effects associated with the ${}^4T_1$ ground term of the octahedral Co^{II} ion, using the T,P isomorphism with an effective orbital moment L = 1; (ii) an axial distortion of the octahedral geometry and (iii) Zeeman interactions. The corresponding Hamiltonian can be written as:[18]

$$\boldsymbol{H} = \left(-\frac{3}{2}\right)\kappa\lambda\boldsymbol{LS} + \Delta\left(\boldsymbol{Lz^2} - \frac{2}{3}\right) + \beta\left[-\left(\frac{3}{2}\right)\kappa\boldsymbol{L}_u + g_e\boldsymbol{S}_u\right]H_u \quad eq.1$$

where u = x, y, z, Δ, as indicated above, is the axial splitting parameter, κ is the orbital reduction factor, and λ is the spin–orbit coupling parameter. The factor -3/2 comes from the fact that the real angular momentum for the $^4T_{1g}$ ground state in an ideal Oh geometry is equal to the angular momentum of the ^4P free ion term multiplied by -3/2. The orbital reduction factor includes the admixing of the $^4T_{1g}(^4P)$ excited term into the $^4T_{1g}(^4F)$ ground term. As indicated elsewhere, the set of nitrogen and oxygen donor atoms around the Co^{II} ion adopts essentially an axially elongated distorted octahedral CoN_3O_3 coordination polyhedron. In such a symmetry, the triplet $^4T_{1g}$ ground state for the hypothetical ideal Oh symmetry splits into an orbital singlet $^4A_2$ and an orbital doublet ^4E. The energy gap between them is described by the axial splitting parameter, Δ. The $^4A_2$ and ^4E levels can undergo an additional split by second order spin-orbit coupling generating two and four Kramers doublets, respectively.[16] When Δ is positive the orbital singlet is the lowest in energy, whereas for negatives values of Δ, the doublet is the ground term.[18, 20] The best fit of the magnetic data of **1** with the above Hamiltonian using the MagSaki[21] software afforded the following parameters: λ= -105 cm^{-1}, κ = 1, Δ = -661 cm^{-1} with an agreement factor $R\chi = 7.0 \times 10^{-5}$. These parameters, which are typical for high-spin octahedral Co^{II}, complexes, support the predicted negative sign of Δ and, consequently, a doublet ^4E ground state for complex **1**. The ground state presents anisotropic *g* values of g_z =7.63 and $g_{x,y}$ = 2.194.

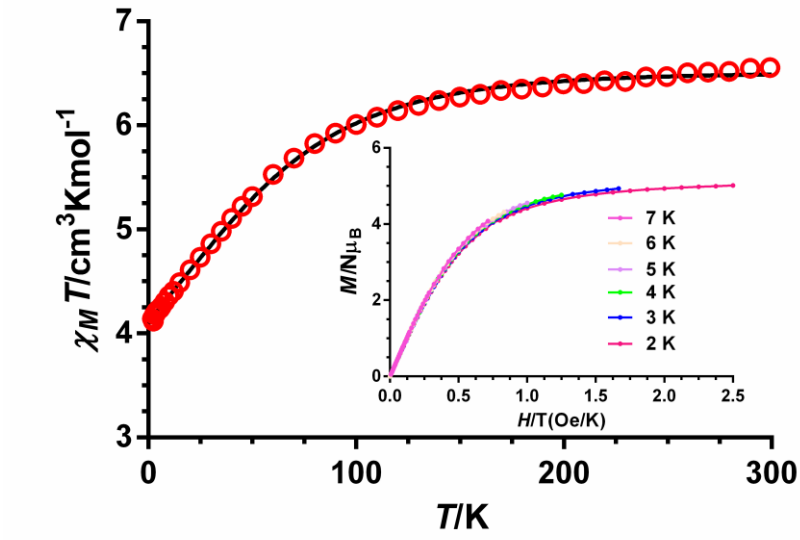

Figure 2.- Temperature dependence of $\chi_M T$ for compound **1**. The solid line represents the best-fit curve using equation 1 (the fit to equation 2 is almost superimposable and is not shown) and *M* vs *H/T* plot for compound **1** (inset).

There is another usual approach to analyze the magnetic data in octahedral high spin Co^{II} complexes, which is based on a phenomenological spin Hamiltonian operating within the S = 3/2 multiplet.[11, 15b, 22] This approach can be used only when Δ is large enough and positive, so that the $^4A_2$ is the ground term and is well separated from the excited ^4E term. The combination of an axial distortion and second-order spin-orbit coupling splits the ^4A ground term in two Kramers doublets Γ_6 and Γ_7. These low-lying Kramers doublets are the only thermally populated and the energy gap between them can be assimilated to a ZFS. The appropriate Hamiltonian to analyse the magnetic properties is as follows:

$$\boldsymbol{H} = D[\boldsymbol{S}_z^2 - S(S+1)/3] + E(\boldsymbol{S}_x^2 - \boldsymbol{S}_y^2) + g\mu_B H\boldsymbol{S} \quad \text{(equation 2)}$$

where S is the spin ground state, D and E are the axial and transverse magnetic anisotropies, respectively, μ_B is the Bohr magneton and H the applied magnetic field and the third term corresponds to the Zeeman interaction. If $E = 0$, then $2D$ represents the energy gap between ±1/2 and ±3/2 Kramers doublets (KD) arising from second order SOC of the quartet ground state. If $D > 0$, the doublet with $M_s = \pm 1/2$ is at lower energy than the doublet with $M_s = \pm 3/2$, whereas when $D < 0$ the reverse distribution of these doublets occurs.

When the system has a ^4E ground state, as in the in the case of **1**, the above Hamiltonian is, in principle, not applicable and then the discussion based on easy-axis anisotropy (D < 0) and easy-plane anisotropy (D > 0) is not appropriate.[23] However, owing to the fact the two lowest Kramers doublets arising from the ^4E term are generally the only populated states at low temperature, the spin Hamiltonian in equation 2 could be used to phenomenologically analyse the magnetic data below ~ 100 K.[15b] In some cases, this spin Hamiltonian is even efficient up to room temperature. It worth mentioning at this point that the temperature dependence of the magnetization at different magnetic fields cannot be used to accurately extract the ZFS parameters of complex **1**, because the *M* vs *H/T* isotherms depend only slightly on temperature below 7 K (see Figure 2 inset). This fact indicates that the *D* value has to be very large, because, in such a case, the thermal depopulation of the low-lying Kramers doublets below 7 K is almost irrelevant and the *M* vs *H/T* curves are almost superimposed. In view of this, the field dependence of the magnetization at different temperatures and the temperature dependence of the magnetic susceptibility of **1** were simultaneously fitted with the above Hamiltonian using

the PHI program (Figure 2).[24] The best fit of the data using an axial *g* tensor led to the following magnetic parameters: D= +80.6 cm^{-1}, E= 7.8 cm^{-1}, g_{xy}= 2.8 and g_z= 2.0 with R= 1.1 x 10^{-8} (R= $\Sigma[(\chi_M T)_{exp.} - (\chi_M T)_{calcd.}]^2/\Sigma((\chi_M T)_{exp})^2$). The energy gap between the ground and first excited Kramers doublets calculated from these parameters is δ = 163.4 cm^{-1}. It is worth noting that unreasonable fits were always obtained when negative sign were used for the initial D values.

In order to support the sign of D, we have carried out low-temperature (down to 5 K) high-frequency and -field EPR (HFEPR) measurements in the 50–650 GHz, and 0–14.5 Tesla range, respectively, on a powder sample of **1** (Figure 3). The observed resonances are of clearly intra-Kramers kind, i.e. they are driven within the *same* Kramers doublet, not *between* different KDs, as witnessed by their field vs. frequency dependence (Figure S2). As to which KD doublet is involved, the simulations in Figure 3 clearly show that it is the m_s= ±1/2 one. This means that the sign of D is positive, and D must be very large, since up to 40 K no thermally-activated resonances within the m_s= ±3/2 KD are detectable (although such a transition would be nominally forbidden (Δm_s= ±3)), it is frequently observed if the zfs rhombicity factor E/D is not exactly equal to zero.[25] The exact value of D is too large to be obtained from HFEPR as no inter-Kramers resonances are detectable but the rhombicity factor could be established, together with the intrinsic *g*-values (see caption to Figure 3). It is worth mentioning that the *g* and $|E/D|$ values are not far from those extracted from the fitting of the susceptibility magnetic data (see above).

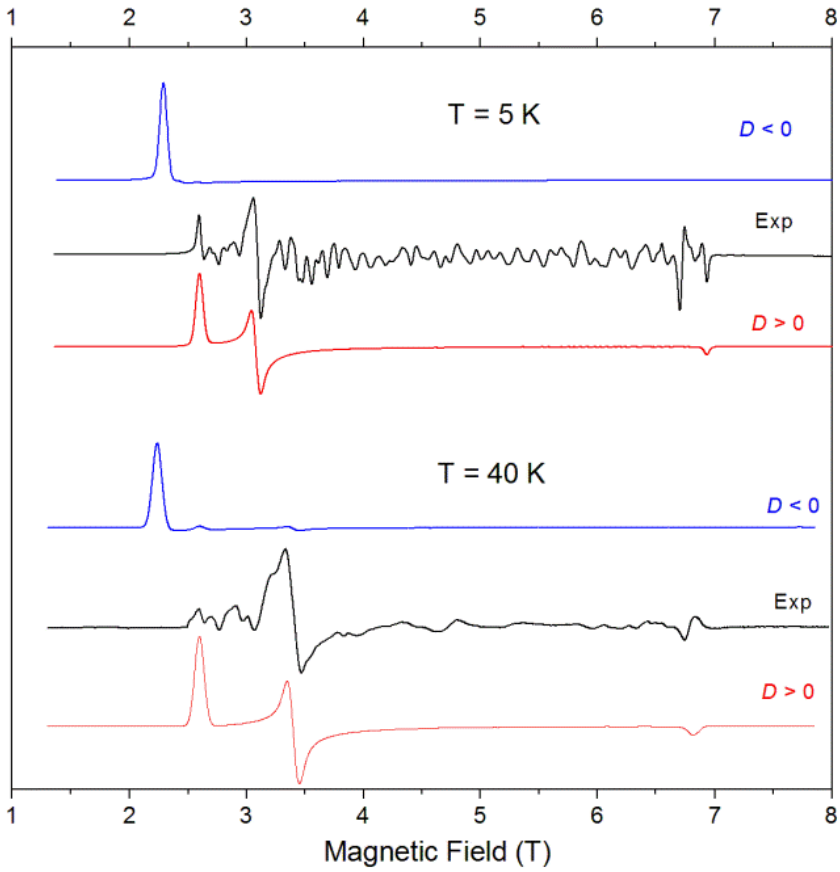

Figure 3. A 101.6 GHz spectra of **1** at 5 and 40 K (black traces) accompanied by simulations using the following parameters: $|E/D| = 0.059$, $g_{\perp} = 2.58$, $g_{\parallel} = 2.12$ (5 K) and $|E/D| = 0.040$, $g_{\perp} = 2.48$, $g_{\parallel} = 2.24$ (40 K). Red traces: $D > 0$; blue traces: $D < 0$. In each case, D was fixed at 93 cm^{-1} (the value obtained by CASSCF + RASSI calculations) and the rhombicity of the zfs tensor was calculated under assumption of an axial g-tensor (i.e. ignoring the possible rhombicity of g-tensor). The "quasi-noise" visible between the turning points is caused by discrete crystallites showing up in the spectrum, despite extensive grinding of the starting material.

The D positive value extracted from magnetic data (spin Hamiltonian in equation 2) is rather larger than those previously reported for the analogous dinuclear complexes [Co(μ-L)(μ-X)$(NO_3)_2$] (X= acetate, benzoate, 9-anthracene carboxylate).[11]

With the aim of underpinning the sign and magnitude of the ZFS for **1**, we have carried out electronic structure CASSCF calculations of the ZFS parameters D and E on the X-ray structure of this complex using MOLCAS and ORCA software packages.[26, 27] The SO-RASSI approach included in MOLCAS gives rise to following ZFS parameters: D= +93.1 cm^{-1}, E= +19.0 cm^{-1} and first excitation energies at spin-free CASSCF level and after the inclusion of the spin-orbit effect of ΔE_1 = 423.1 cm^{-1} and δ = 197.6 cm^{-1}, respectively. The quasi-degenerate perturbation

theory (QDPT) approach implemented in ORCA gives rise to: D = +93.4 cm^{-1}, E = +21.5 cm^{-1}, ΔE_1 = 411.6 cm^{-1} and δ = 201.0 cm^{-1}. The computed values are very similar with both procedures and slightly larger than the obtained experimentally. It is not surprising, as it was observed before, that the employed methodology overestimated the D values for the family of $Co^{II}Y^{III}$ complexes indicated above.[11] The differences might be due to the intrinsic limitations of the employed method, possible small changes on the Co^{II} coordination geometry at very low temperature and the inaccuracy of the fitting of the magnetic data.

The S = 1/2 effective g-values calculated for the ground Kramers doublet using MOLCAS (g_x = 2.18, g_y = 3.60, g_z = 7.23), indicate that this state is highly anisotropic. These g values reproduce reasonably well the experimental magnetization by using an effective S = 1/2 spin model, thus supporting an isolated ground state. Nevertheless, the fact that the S = 3/2 g-values extracted from the HFEPR spectra cannot be well reproduced with the above-calculated S =1/2 effective g values[28] suggest that the ZFS Hamiltonian, as indicated elsewhere, is a too crude model to analyze the magnetic properties of this compound and therefore the extracted D value should be taken with caution. It should be noted that the calculated S =1/2 effective g values are very similar to those obtained for other Co^{II} complexes with a ^{4}E ground state.[23b] The principal direction of the g_z value is close to the $O_{carbonate}$-Co-N axis (Figure 4), whereas the directions of g_x and g_y are in the plane perpendicular to this axis bisecting the angles formed by the donor atoms of the ligands. This fact suggests that, as expected, the bonding and electronic structure of the ligands play an important role in dictating the g-values. The shortest Co-$O6_{carbonate}$ bond is probably responsible for the direction of the easy anisotropic axis. The fact that the easy axis does not lie along the distortion axis but along the shortest Co-donor bonds has been previously observed in other mononuclear Co^{II} complexes.[23b]

It is worth noting that the sign and magnitude of D can be predicted by evaluation of the D_{ii} components (i = x,y,z), which depend inversely on the energy of the d-orbitals, specifically on the excitation energies, as well as of the m_l values of the orbitals involved in the lowest energy transitions.[8] Thus, to have a positive contribution to the D value the excitation energy should involve two orbitals with $m_l = \pm 1$. In the same way than for the previously reported family of CoY complexes,[11] there is a strong and positive contribution from the two first quartets to the D value of **1** (Table S4). That allows us to rationalize that the distortion in **1** gives rise to a splitting of the t_{2g} orbitals, where the d_{xy} should be lower in energy than the d_{yz} and d_{yz} orbitals, which must be degenerated or close in energy (one of them double-occupied and the other one semi-occupied). This splitting of the d orbitals is in agreement with the ^{4}E ground term. It should be noted that the same splitting of the t_{2g} orbitals has been calculated for a Co^{II} complex with

similar distortions from the ideal Oh geometry.[16a] As the energy gap between the dxy orbital and dxz, dyz orbitals, provoked by the distortion of the octahedral geometry, should be small, from a qualitative point of view, a large *D* positive value is expected for this compound, which match well with the experimental and theoretical results.

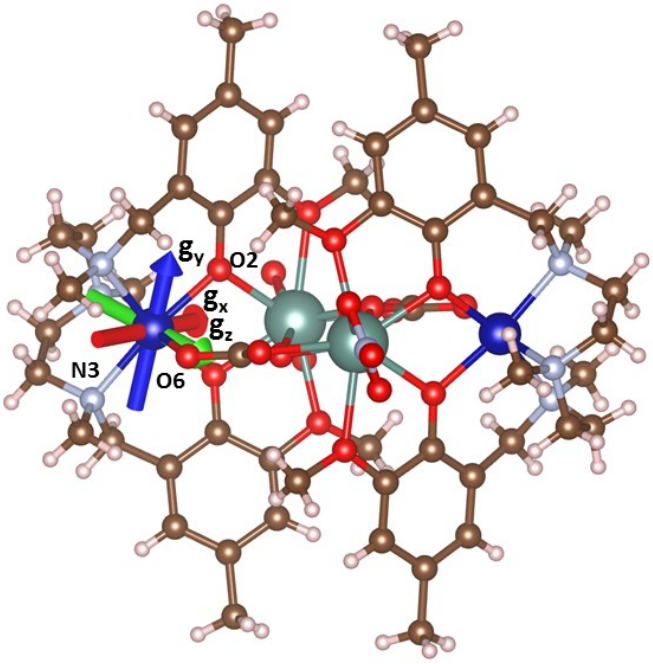

Figure 4.- Orientation of the principal axes for the S = 1/2 effective g values of the ground Kramers doublet of **1**.

We have previously reported the existence of a non-linear correlation between the *ab initio* calculated *D* values for the closely related $[Co(\mu\text{-}L)(\mu\text{-}X)Y(NO_3)_2]$ dinuclear complexes (X= acetate, benzoate, 9-anthracene carboxylate), that only differ in the ancillary bridging ligand.[11b] For these complexes, the *D* value decreases with the increase of the distortion from the octahedral geometry quantified by the shape measures parameter (S). The Co^{II} ions in **1** are well separated in the structure (> 8 Å), so that dipolar and magnetic interactions, if exist, can be considered as negligible. Therefore, from the magnetic point of view, complex **1** can be considered as two non-interacting $Co^{II}Y^{III}$ isolated dinuclear units analogous to that of the $[Co(\mu\text{-}L)(\mu\text{-}X)Y(NO_3)_2]$ complexes and therefore should obey the above indicated magneto-structural correlation. In fact, complex **1** exhibiting the lower S value (1.44) shows the higher *D* value (see Figure 5).

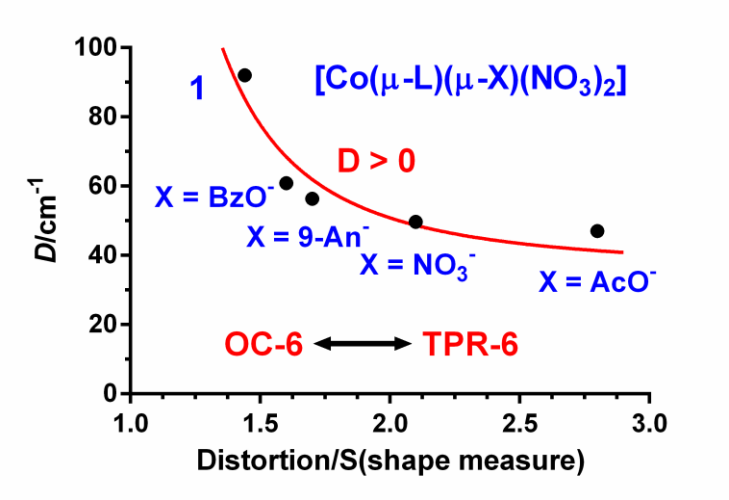

Figure 5.- Correlation between *D* and the distortion from the octahedral geometry quantified by the shape measures parameter (S).

Dynamic ac magnetic properties

In order to know if complex **1** shows slow magnetization relaxation and to compare the results with those for the $[Co(\mu\text{-}L)(\mu\text{-}X)Y(NO_3)_2]$ dinuclear complexes, dynamic *ac* magnetic susceptibility measurements were performed under a 3.5 Oe alternating field. Complex **1** does not show any out-of-phase signals (χ''_M) above 2 K at zero applied dc field. This fact is not surprising because, as it has been recently shown for Kramers ions like Co(II) with D > 0, the electronuclear spin states arising from the hyperfine interactions have negligible magnetic moments at zero field, so that slow relaxation cannot be observed. However, in the presence of an applied *dc* field, the electronuclear spin states acquire magnetic moment and, if the compound behave as a SMM, slow relaxation could be observed.[9] It has been recently shown that, even in these conditions, some compounds do not exhibit slow relaxation because the transversal magnetic field created by intermolecular interactions could split the Kramers doublet states opening relaxation pathways for direct and QTM processes.[11a] In these cases, to observe magnetization relaxation, magnetic dilution with an isostructural diamagnetic counterpart to partly or fully suppress intermolecular interactions, is required.

To analyze the dynamic behavior of **1**, the field dependence of the *ac* magnetic susceptibility measurements at T= 2 K, for magnetic fields varying between 0.025 and 0.20 T, were undertaken. The aim was not only to know if compound **1** exhibits field induced slow magnetization relaxation, but also to investigate how it evolves with the applied magnetic field. After application of a dc magnetic field, compound **1** shows strong frequency dependent out-of-phase signals below 10 K (Figure 6). Nevertheless, none of them exhibit clear maxima above 2 K in the 10-1500 Hz frequency range. It is worth mentioning that below 0.05 T almost only

one relaxation process is observed, whereas for $H_{dc} > 0.1$ T, a second and slower relaxation process begins to appear. We have extracted the relaxation times at different fields for the fast relaxation process (Figure 6) by fitting the frequency dependence of the out-of-phase signal to the Debye model. As it can be observed in Figure 6, $1/\tau$ increases with the increase of the field following a $1/\tau$ *vs* H^4 law, which is typical of a direct process. Therefore, it seems that, at low temperature, **1** does not show QTM but a direct relaxation process.

It is worth mentioning that the two relaxation processes can be clearly observed for $H_{dc} = 0.2$ T (see Figure S8). The slow field induced relaxation process is rather usual in SMMs that are exposed to a magnetic field and it has been suggested that its origin can be found in either: (i) a spin-phonon direct relaxation process promoted by the split of the Kramers degeneration when a magnetic field is applied (the larger is the energy gap between the two m_s ground states, the higher is the phonon density with an energy equal to this gap),[29] or (ii) intermolecular interactions.[30]

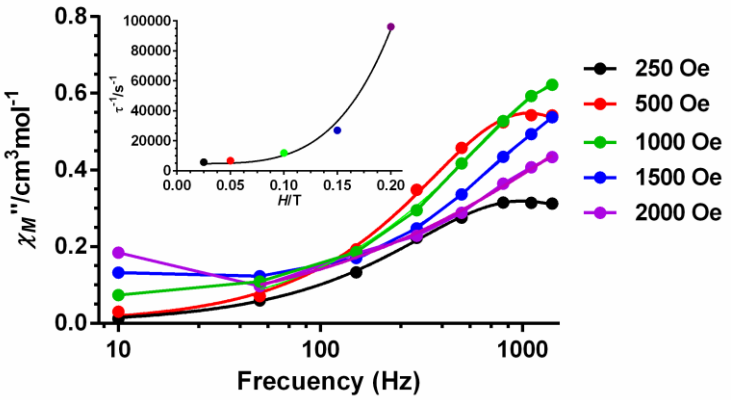

Figure 6.- Field dependence of the out-of-phase signal (χ''_M) at 2 K. Inset: Field dependence of the relaxation times at 2 K..

Temperature and frequency ac measurements were carried out under a small static field of 0.025 T to avoid the appearance of the field induced relaxation process. The strong intensity of the signals corresponding to the direct process at low temperature modulates the intensity of the signals at higher temperatures, so that no clear maxima are observed and only an incipient shoulder appears above 4 K in the temperature dependence of the χ''_M plots at different frequencies (Figure S4). The ac data could not be correctly fitted to the Debye model because the peaks lie above the studied frequency range (Figure S3). Nevertheless, we have used an alternative approach to extract the relaxation parameters from the ac data. The ratio between

the out-of-phase and in phase *ac* susceptibility can be expressed in an approximate manner as $\chi''_M/\chi'_M = 2\pi f\tau$ (equation 3).[31] The replacement in this equation of the relaxation time (τ) by its expression for each relaxation mechanism would allow extracting the corresponding relaxation parameters. If we assume that hypothetically the relaxation takes place exclusively through an Orbach relaxation mechanism, for which $\tau = \tau_0 \exp(-U_{eff}/k_BT)$, the following equation would became:

$$\ln(\chi''_M/\chi'_M) = \ln(2\pi f\tau_0) - U_{eff}/k_BT \text{ (equation 4)}$$

The energy barrier could be approximately estimated by fitting of the experimental χ''/χ' data in the high frequency region to equation 4. The best fit at different frequencies (Figure 7) leads to the following parameters: $U_{eff}/k_B \approx 7.9$ K and $\tau_0 \approx 4.6\times10^{-6}$ s. The extracted U_{eff} value is much lower that the experimental energy gap between the ground S= ±1/2 and the excited state S= ±3/2 extracted from static susceptibility measurements. This result once again confirms that the magnetization reversal for field induced Co^{II} SIMs with D > 0 does not take place through an Orbach process but through direct and Raman processes, which predominate at low at high temperatures, respectively.[11b]

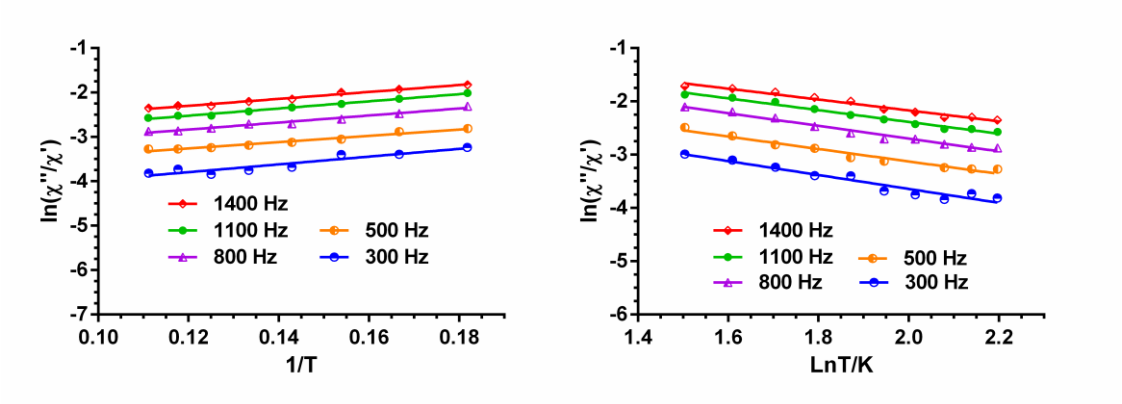

Figure 7.- Temperature dependence of the ratio of the in-phase and out-of-phase *ac* components at different frequencies under a magnetic field of 0.025 T. Solid lines correspond to the fit of the experimental data to equation 4 (left) and equation 5 (right).

In view of the fact that at high temperatures the relaxation must proceed through a Raman process, we have fitted the χ''/χ' data to the following equation:

$$\ln(\chi''_M/\chi'_M) = \ln(2\pi fC) - n(\ln T) \text{ (equation 5)}$$

where in equation 3, τ has been replaced by the power law $\tau^{-1} = CT^n$. The data in the 5.5 - 9.5 K range were fitted to the equation 5 using frequencies between 300 and 1400 Hz. The fitting procedure led to the following parameters: $C = 0.00014\ s^{-1}K^n$ and n= 1.16. Although n= 9 for Kramers ions,[32] however, if both, acoustic and optical phonons, are taken into account, n values between 1 and 6 can be considered as acceptable.[33] Therefore, it is clear that the Raman process dominates at high temperature and low fields for the fast relaxation process.

In order to know how the dynamic relaxation parameters evolve with the magnetic field, we have taken ac susceptibility measurements under a static magnetic field of 0.20 T (Figures S6-S9). It is of interest that the overall dynamic behavior is similar to that observed under 0.025 T, but the relaxation parameters change to the following values: $U_{eff}/k_B \approx 17.2$ K and $\tau_0 \approx 6.6\times10^{-7}$ s using equation 4 and $C = 0.005\ s^{-1}K^n$ and n= 2.18 for equation 5. In view of these results, it appears that the Raman process slows down by increasing the static magnetic field. Compared to the analogous $Co^{II}Y^{III}$ dinuclear complexes $[Co(\mu\text{-}L)(\mu\text{-}X)Y(NO_3)_2]$ (X= nitrato, benzoato, acetato, 9-antharcenecarboxylato),[11] the dynamic behaviour of **1** is quite different. Thus, the dinuclear complexes $[Co(\mu\text{-}L)(\mu\text{-}X)Y(NO_3)_2]$ (X= nitrate and acetate) exhibit fast QTM, which is almost suppressed in the presence of a field of 0.1 T, so that clear maxima appear in the temperature and frequency dependence of the out-of-phase component of the ac susceptibility in the 2 -6 K temperature range. On the other hand, the complexes $[Co(\mu\text{-}L)(\mu\text{-}X)Y(NO_3)_2]$ (X= benzoate and 9-anthracenecarboxylato)[11b,c] do not show any out-of-phase signal even in the presence of magnetic field and need to be magnetically diluted to suppress intermolecular interactions and to observe slow relaxation.[11b,c] This is due to the existence of strong intermolecular interactions that favour the fast QTM. The dilution process suppresses intermolecular interactions and then field-induced neat maxima are also observed in the 2-6 K range in the χ''_M *vs* T plot at different frequencies. In spite of the absence of significant intermolecular interactions in **1** (Co···Co distance is larger than 8.0 Å and there are no $\pi\cdots\pi$ interactions), and in contrast to the $Co^{II}Y^{III}$ dinuclear complexes $[Co(\mu\text{-}L)(\mu\text{-}X)Y(NO_3)_2]$ (X= nitrate and acetate), the temperature and frequency dependence of χ''_M of **1** does not show any neat maximum after applying magnetic fields up to 0.2 T, either in diluted or pristine forms. Instead, as indicated elsewhere, a strong signal appears at very low temperature (below 4 K), which does not arise from QTM but from either a spin-phonon direct process or intermolecular dipolar interactions (see Figure S4).

It should be pointed out that, sometimes, the application of a magnetic field on octahedral Co^{II} complexes promotes the emergence of two well-differentiate relaxation processes, one of them originated from dipolar intermolecular interactions.[30] Interestingly, this latter relaxation process disappears in some cases with the increase of the magnetic field and in other cases when the magnetic field decreases. As expected, this relaxation process due to intermolecular dipolar interactions disappears in the magnetic diluted complexes. However, the magnetic diluted complex **1'** (with a Zn/Co =10/1 magnetic site dilution) shows a similar behaviour to **1** (Figure S10), pointing out the single-ion origin of the magnetic relaxation.

It has recently shown, from experimental and theoretical results, that the temperature dependence of the spin relaxation depends on the electronic structure as well as the vibrational characteristics of the specific SMM.[34] Therefore, the frequency and lifetime of phonons together with spin-phonon coupling coefficients strongly affect the relaxation time. In this regard, internal vibrations play an essential role in connecting the spin states and phonons that contribute to the spin-relaxation pathways. Nevertheless, only a few local vibrational modes with the lowest frequency are active at low temperature. The reduction of the molecular size should favour the decreasing of the relaxation rate because there will be less degrees of freedom that can combine with the local vibrations.[35] Moreover, it has been suggested that the direct relaxation between two quasi-degenerate ground states is accelerated in structurally flexible SMMs.[34] In view of the above considerations, it is not unexpected that the tetranuclear $Co^{II}_2Y^{III}_2$ compound, which is larger and flexible than the dinuclear $Co^{II}Y^{III}$ counterparts, exhibits a persistent and intense direct relaxation process at low temperature.

Finally, in this context, we would like to remark that among the family of $[Co(\mu\text{-}L)(\mu\text{-}X)Y(NO_3)_2]$ (X = acetate, nitrate, benzoate and 9-anthracenecarboxylato) complexes, those bridging ligands containing large rigid groups such as benzoate and anthracenecarboxylate exhibits larger values of the phenomenological U_{eff} parameters (33.2 K and 34.6 K, respectively) than those with acetate or nitrate bridging groups (27.1K and 24.8 K). The rigid network of π-staking interactions existing in the former compounds could be presumably responsible for slower relaxation observed for them.

Nevertheless, more examples of similar compounds with different size and flexibility are needed to support the above hypotheses.

Conclusions

The compartmental ligand N,N',N''-trimethyl-N,N'-bis(2-hydroxy-3-methoxy-5-methylbenzyl)diethylenetriamine has been successfully used to prepare a new $Co^{II}_2Y^{III}_2$ complex. In this compound, the centrosymmetric $Co^{II}_2Y^{III}_2$ tetranuclear entity is made of two $[Co(\mu\text{-}L)Y(NO_3)_3]$ dinuclear units connected by two carbonate bridging ligands with κ^2-O,O':κ-O:κO'' tetradentate coordination mode. The calculated *ab initio* axial anisotropy parameter (*D*) in this family of dinuclear and tetranuclear $Co^{II}_nY^{III}_n$ complexes correlates with the distortion of the CoN_3O_3 coordination polyhedron from the ideal octahedral geometry to trigonal prismatic, so that *D* decreases with increasing the distortion from octahedral geometry. Among the $Co^{II}_nY^{III}_n$ complexes, the reported $Co^{II}_2Y^{III}_2$ compound exhibits the lower distortion from the ideal octahedral geometry and therefore the larger anisotropy (D = +82.6 cm^{-1}). It should be noted that the ZFS splitting Hamiltonian is not appropriate when the system has a ^4E ground state, as in the case of $Co^{II}_2Y^{III}_2$, and therefore the extracted *D* value has to be taken with caution. As expected, there is no correlation between the *D* value and the magnetization dynamics for this family of $Co^{II}_nY^{III}_n$ complexes, thus confirming that the magnetization reversal takes place through relaxation processes others than the Orbach one.

Under a static magnetic field of 0.025 T, the $Co^{II}_2Y^{III}_2$ complex almost shows only one relaxation process, which does not exhibits QTM but a direct relaxation process at very low temperature, whereas, at higher temperatures, the Raman spin-phonon relaxation process is dominant. However, at H_{dc} = 0.2 T, this complex shows two relaxation processes: (i) the slow one, induced by the magnetic field, that can be associated to a spin-phonon direct relaxation process promoted by the split of the Kramers degeneration when a magnetic field is applied and (ii) a Raman spin-phonon relaxation process. This latter is similar to that observed under 0.025 T, but slows down by increasing the static magnetic field.

The fact that the Raman relaxation process for the $Co^{II}_2Y^{III}_2$ complex is faster that those observed for the $Co^{II}Y^{III}$ dinuclear counterparts, as well as the persistence of the direct process at low temperature under different static magnetic fields and after magnetic dilution, could presumably be a consequence to the larger size and flexibility of the former molecule with respect to the latter ones.

Experimental

Synthetic procedures

General Procedures: Unless stated otherwise, all reactions were conducted in oven-dried glassware in aerobic conditions, with the reagents purchased commercially and used without further purification. The H_2L ligand was prepared as previously reported.[36]

Synthesis of [{Co(μ-L)Y(NO_3)}$_2$(μ-CO_3)$_2$]·2CH_3OH·2H_2O (1): To a solution of the ligand (0.056 g, 0.125 mmol) in methanol (15 ml) was subsequently added with continuous stirring $Co(NO_3)_2·6H_2O$ (0.036 g, 0.125 mmol), $Y(NO_3)_3·6H_2O$ (0.048 g, 0.125 mmol) and triethylamine (0.025g, 0.25 mmol). Then, a solution of Na_2CO_3 (0.026 g, 0.25 mmol) in the minimum quantity of water was added dropwise and stirred for 5 minutes. The brown-pink solution was filtered to eliminate any amount of insoluble material and allowed to stand at room temperature. After three days, pink crystals suitable for X-ray diffraction were obtained. Yield: 47 %. Anal. Found: C, 42.86; H, 5.10; N, 7.42. Anal. Calc. for $C_{54}H_{82}N_8O_{24}Co_2Y_2$: C, 42.59; H, 5.43; N, 7.36. IR (cm^{-1}): 3018, $\nu(CH)_{aromatic}$; 2969(w), 2965(w), 2839(w) ν(CH); 1548 (s), 1345 (s) $\nu(CO)_{carbonate}$.

Syntheses of the diluted sample 1'. This compound was prepared following the same method as for **1**, but using a 1:10 Co/Zn ratio, that is 3.63 mg (0.0125 mmol) of $Co(NO_3)_2·6H_2O$ and 33.46 mg (0.1125 mmol) of $Zn(NO_3)_2·6H_2O$. From the resulting solution a pale pink microcrystalline precipitated. The X-ray powder spectrum demonstrates that this compound is isostructural with the undiluted complex (see Figure S11).

Physical measurements

Elemental analyses were performed at the "Centro de InstrumentacionCientifica" (University of Granada) on a Fisons-Carlo Erba analyser model EA 1108. IR spectra on powdered samples were recorded with a Thermo Nicolet IR200FTIR using KBr pellets.

Variable-temperature (2−300 K) magnetic susceptibility measurements on polycrystalline samples of **1**and **1′** under an applied field of 1000 Oe were carried out with a Quantum Design SQUID MPMS XL-5 device. Alternating-current (ac) susceptibility measurements under different applied static fields were performed using an oscillating ac field of 3.5 Oe and ac frequencies ranging from 10 to 1500 Hz. The experimental susceptibilities were corrected for the sample holder and diamagnetism of the constituent atoms using Pascal's tables. A pellet of the sample cut into very small pieces was placed in the sample holder to prevent any torquing of the microcrystals.

HFEPR measurements were performed at the NHMFL at several subterahertz frequencies between 50 and 650 GHz and low temperatures on loose powders and pellets, using an instrument described previously in detail[37] with the exception of a Virginia Diodes subterahertz

wave source, consisting of a 13 ± 1 GHz frequency generator and a cascade of amplifiers and frequency multipliers.

The X-ray powder diffraction (XRPD) spectra were registered on a (2θ) Bruker D2-PHASE using CuKα (λ = 1.5418 Å) radiation and LINXEYE detector, from 5 to 50 º (2θ) at a scanning rate of 0.5 º 2θ/min.

Single-Crystal Structure Determinations.

Suitable crystals of **1**were mounted on a glass fibre and used for data collection. X-ray diffraction data of **1** were collected at 110 K using a Bruker AXS SMART APEX CCD diffractometer (MoK_α radiation, λ= 0.71073 Å) outfitted with a CCD area-detector and equipped with an Oxford Cryosystems 700 series Cryostream device. Unit-cell parameters were determined and refined on all observed reflections using APEX2 software.[38] Correction for Lorentz polarization and absorption were applied by SAINT and SADABS programs, respectively.[39,40]

The structures were solved by direct methods and refined by the full-matrix least-squares method onF^2 using the SHELX software suite and SHELXL-2014 program.[41] All non-hydrogen atoms were refined anisotropically. Hydrogen atom positions were calculated and isotropically refined as riding models to their parent atoms. Solvent methanol molecules are disordered over two positions with site occupancies refining to 0.548 (10) and 0.452 (10). A summary of selected data collection and refinement parameters can be found from the Supporting Information (Table S1) and CCDC 1912162.

Computational methodology

Zero-field splitting parameters (D and E) were calculated using two different software packages, MOLCAS[26] (along with Single Aniso) and ORCA.[27] The crystal structure was employed for the calculations and one of the Co^{2+} ions was substituted by a diamagnetic Zn^{2+} ion. We have used MOLCAS (along with the SINGLE_ANISO [42] code) and then the SO-RASSI (Restricted Active Space State Interaction) approach was employed to mix them and obtain the final energy states. We have employed an all electron ANO-RCC basis set:[43] Co (6s5p4d2f), Y (5s4p3d1f), Zn (5s4p3d1f), N (4s3p2d1f), C (3s2p) and H (2s). Similar CASSCF calculations were performed with ORCA.[27] In this case spin-orbit effects were included using the quasi-degenerate perturbation theory (QDPT) and scalar relativistic effects were taken into account using the DKH (Douglas-Kroll-Hess) procedure.[44] We have employed def2-TZVPP basis set,[45] including the auxiliary basis sets for correlation and Coulomb fitting, for all the atoms. In both cases the employed active space includes seven electrons in five 3d-orbitals of Co(II) CAS (7,5). We have included all 10 states for the 2S+1= 4 (quartet) states arising from

the ^{4}F and ^{4}P terms of Co(II), and all the 40 states for the respective 2S+1= 2 (duplet) states arising from the ^{2}P, ^{2}D (twice), ^{2}F, ^{2}G and ^{2}H terms of the Co(II) ion.

Acknowledgements

Financial support from Ministerio de Economía y Competitividad (MINECO) for Project CTQ2014-56312-P and for a Maria de Maeztu grant (MDM-2017-0767) and Ministerio de Educación, Cultura y Deporte for projects PGC2018-093863-B-C21 and PGC2018-102052-B-C21, the Junta de Andalucía (FQM-195) and the Project of excellence P11-FQM-7756), the University of Granada and the Generalitat de Catalunya (SGR2017-1289). M.A. P. thanks to MINECO for a Juan de la Cierva Incorporation contract (IJCI-2014-19485). E.R. thanks the Generalitat de Catalunya for an ICREA Academia fellowship and CSUC for computational resources. S.G.-C. thanks Generalitat de Catalunya for a Beatriu de Pinós Fellowship (2017 BP 00080). The HFEPR studies were supported by the NHMFL, which is funded by the National Science Foundation (Cooperative Agreement DMR 1157490) and the State of Florida. The authors thank Dr. A. Ozarowski (NHMFL) for his EPR software SPIN.

References

1. (a) D. Gatteschi and R. Sessoli, *Angew. Chem. Int. Ed.,* 2003, **42**, 268; (b) *Molecular Nanomagnets,* Ed. D. Gatteschi, R. Sessoli and J. Villain, Oxford University Press, Oxford, 2006; (c) *Molecular Magnets: Physics and Applications*, Ed. J. Bartolomé, F. Luis and J. F. Fernández, Springer-Verlag, Berlin-Heidelberg, 2014; (d) S. Gao, *Structure and Bonding*, Springer-Verlag, Berlin-Heidelberg, 2015, vol. **164**.

2. (a) M. N. Leuenberger and D. Loss, *Nature*, 2001, **410**, 789; (b) A. R. Rocha, V. M. García-Suárez, S. W. Bailey, C. J. Lambert, J. Ferrer and S. Sanvito, *Nat. Mater*., 2005, **4**, 335; (c) A. Ardavan, O. Rival, J. L. Morton, S. J. Blundell, A. M. Tyryshkin, G. A. Timco and R. E. P. Winpenny, *Phys. Rev. Lett*., 2007, **98**, 057201; (d) L. Bogani and W. Wernsdorfer, *Nat. Mater.*, 2008, **7**, 179; (e) E. Coronado and A. Epstein , *J. Mat. Chem.,* 2009, **12**, 1661; (f) M. J. Martínez-Pérez, S. Cardona-Serra, C. Schlegel, F. Moro, P. J. Alonso, H. Prima-García, J. M. Clemente-Juan, M. Evangelisti, A. Gaita-Ariño, J. Sesé, J. Van Slageren, E. Coronado and F. Luis, *Phys. Rev. Lett.,* 2012, **108**, 247213. (g) G. Aromí, D. Aguilà, P. Gamez, F. Luis and O. Roubeau, *Chem. Soc. Rev*., 2012, **41**, 537; (h) R. Vincent, S. Klyatskaya, M. Ruben, W. Wernsdorfer and F. Balestro, *Nature*, 2012, **488**, 357; (i) M. Ganzhorn, S. Klyatskaya, M. Ruben and W. Wernsdorfer, *Nat. Nanotechnol*., 2013, **8**, 165; (j) M. Jenkins, T. Hümmer, M. J. Marínez-Pérez, J. García-Ripoll, D. Zueco and F. Luis, *New J. Phys*., 2013, **15**, 095007; (k)

E. Coronado and M. Yamashita, *Dalton Trans*., 2016, **45**, 16553; (l) J. Escalera-Moreno, J. Baldoví, A. Gaita-Ariño and E. Coronado, *Chem Sci.,* 2018, **13**, 3265; (m) M. Atzori, S. Benci, E. Morra, L. Tesi, M. Chiesa, R. Torre, L. Sorace and R. Sessoli, *Inorg Chem*., 2018, **57**, 731; (n) L. Tesi, E. Lucaccini, I. Cimatti, M. Perfetti, M. Mannini, M. Atzori, E. Morra, M. Chiesa, A. Caneschi, L. Sorace and R. Sessoli, *Chem Sci.,* 2016, **7**, 2074.

3. (a) G. Aromi and E. K. Brechin, *Single-Molecule Magnets and Related Phenomena*, ed. R. Winpenny, *Struct. Bond*. 2006, **122**, 1, Springer-Verlag, Berlin-Heidelberg; (b) R. Layfield, M. Murugesu, *Lanthanides and Actinides in Molecular Magnetism*. Wiley-VCH, 2015; (c) D. N. Woodruff, R. E. P. Winpenny, R. A. Layfield, *Chem. Rev*., 2013, **113**, 5110

4. (a) F. Neese and D. A. Pantazis, *Faraday Discuss*., 2011, **148**, 229; (b) O. Waldmann, *Inorg. Chem.,* 2007, **46**, 10035.

5. (a) O. Waldmann, A. M. Ako, H. U. Gudel and A.K. Powell, *Inorg. Chem*., 2008, **47**, 3486; (b) A. J. Tasiopoulos, A. Vinslava, W. Wernsdorfer, K. A. Abboud and G. Christou, *Angew. Chem. Int. Ed.,* 2004*,* **43**, 2117.

6. (a) C. A. P. Goodwin, F. Ortu, D. Reta, N. F. Chilton and D. P. Mills, *Nature,* 2017, **548**, 439; (b) F. S. Guo, B. M. Day, Y. C. Chen, M. L. Tong, A. Mansikkamäki and R. A. Layfield, *Angew. Chemie Int. Ed.,* 2017, **56**, 11445. (c) F. S. Guo, B. M. Day, Y. C. Chen, M. L. Tong, A. Mansikkamäki and R. A. Layfield, *Science* 2018, **362**, 1400.

7. L. Norel, L. E. Darago, B. Le Guennic, K. Chakarawet, M. I. Gonzalez, J. H. Olshansky, S. Rigaut and J. R. Long, *Angew. Chemie Int. Ed.*, 2018, **57**, 1933.

8. S. Gómez-Coca, E. Cremades, N. Aliaga-Alcalde. E. Ruiz, *J. Am. Chem. Soc*., 2013, **135**, 7010.

9. S. Gómez-Coca, A. Urtizberea, E. Cremades, P. J. Alonso, A. Camón, E. Ruiz and F. Luis, *Nat. Commun*., 2014, **5**, 4300.

10. (a) G. A.Craig and M. Murrie, *Chem. Soc. Rev*., 2015, **44**, 2135; (b) A. K. Bar, C. Pichon and J. P. Sutter, *Coord. Chem. Rev*., 2016, **308**, 346; (c) S. Gómez-Coca, D. Aravena, R.Morales and E. Ruiz, *Coord. Chem. Rev.,* 2015, **289-290**, 379; (d) J. M. Frost, K. L. M. Harriman, and M. Murugesu, *Chem. Sci.,* 2016, **7**, 2470; (e) M. Feng and M-.L. Tong, *Chem. Eur. J.,* 2018, **24**, 7574; (f) D. Maniaki, E. Pilichos and S. P. Perlepes, *Front. Chem,.* 2018, **6**, 461. (g) S. Tripathi, A. Dey, M. Shanmugam, R. S. Narayanan, V. Chandrsekhar, *Top Organomet Chem* Berlin, Heidelberg, 2018.

11. (a) E. Colacio, J. Ruiz, E. Ruiz, E. Cremades, J. Krzystek, S. Carretta, J. Cano, T. Guidi, W. Wernsdorfer and E. K Brechin, *Angew. Chem., Int. Ed*., 2013, **52**, 9130; (b) M. A. Palacios, J. Nehrkorn, E. A. Suturina, E. Ruiz, S. Gómez-Coca, K. Holldack, A.

Schnegg, J. Krzystek , J. M Moreno and E. Colacio, *Chem. Eur. J.*, 2017, **23**, 11649; (c) E. Colacio, Mannich Base Ligands as Versatile Platforms for SMMs. In: *Topics in Organometallic Chemistry*. Springer, Berlin, Heidelberg, 2018.

12. S. Titos-Padilla, J. Ruiz, J. M. Herrera, E. K. Brechin, W. Wersndorfer, F. Lloret and E. Colacio, *Inorg Chem.,* 2013, **52**, 9620.

13. M. Llunell, D. Casanova, J. Cirera, P. Alemany, S. Alvarez, SHAPE, version 2.0; Universitat de Barcelona: Barcelona, Spain, 2010.

14.- Y. Dou, *J. Chem. Educ*.1990, **67**, 134.

15.- (a) A. B. P. Lever, *J. Chem. Ed.* 1968, **45**, 710. (b) A. Świtlicka, J. Palion-Gazda, B. Machura, Joan Cano, F. Lloret and Miguel Julve, *Dalton Trans*., 2019, **48**,1404.

16.- (a) H. Sakiyama, R. Sudo, T. Abiko, D. Yoshioka, R. Mitsuhashi, M. Omote, M. Mikuriya, M. Yoshitakec and M. Koikawa, *Dalton Trans*., 2017, **46**, 16306. (b) J. Titis and R. Boča, *Inorg. Chem*. 2011, **50**, 11838.

17.- B. N. Figgis and M. A. Hitchman, *Ligand Field Theory and its Application*, Wiley-VCH, 2000.

18. F. Lloret, M. Julve, J. Cano, R. Ruiz-García and E. Pardo, *Inorg. Chim. Acta*, 2008, **361**, 3432.

19.- S. Alvarez, S., D. Avnir, M. Llunell and M. Pinsky. *New J. Chem*., 2002, **26**, 996.

20.- D. V. Korchagin, A. V. Palii, E. A. Yureva, A. V. Akimov, E. Y. Misochko, G. V. Shilov, A. D. Talantsev, R. B. Morgunov, A. A. Shakin, S. M. Aldoshin and B. S. Tsukerblat, Dalton Trans., 2017, **46**, 7540.

21.- H. Sakiyama, *J. Comput. Chem., Jpn*., 2007, **6**, 123.

22.- D. Sertphon, K. S. Murray, W. Phonsri, J. Jover, E. Ruiz, S. G. Telfer, A. Alkas, P. Harding, and D. J. Harding, *Dalton Trans.* 2018, **47**, 859.

23.-(a) E. A. Buvaylo, V. N. Kokozay, O. Y. Vassilyeva, B. W. Skelton, A. Ozarowski, J. Titiš, B. Vranovičová, and R. Boča, *Inorg. Chem.* 2017, **56**, 6999; (b) J. P. S. Walsh, G. Bowling, A.-M. Ariciu, N. F. M. Jailani, N. F. Chilton, P. G.Waddell, D. Collison, F. Tuna and L. J. Higham, *Magnetochemistry* 2016, **2**, 23.

24. N. F. Chilton, R. P. Anderson, L. D. Turner, A. Soncini and K. S. Murray, *J. Comput. Chem.,* 2013, **34**, 1164.

25. S. Sottini, G. Poneti, S. Ciattini, N. Levesanos, E. Ferentinos, J. Krzystek, L. Sorace, and P. Kyritsis, *Inorg. Chem.* 2016, **55**, 9537.

26. (a) J. A. Duncan, *J. Am. Chem. Soc*., 2009, **131**, 2416; (b) F. Aquilante, L. De Vico, N. Ferre, G. Ghigo, P. A. Malmqvist, P. Neogrady, T. B. Pedersen, M. Pitonak, M. Reiher, B. O. Roos, L. Serrano-Andres, M. Urban, V. Veryazov and R. Lindh, *J. Comput. Chem*., 2010, **31**, 224; (c) V. Veryazov, P. O. Widmark, L. Serrano Andres, R. Lindh and B. O. Roos, *Int. J. Quantum Chem*., 2004, **100**, 626; (d) G. Karlstrom, R. Lindh, P. A. Malmqvist, B. O. Roos, U. Ryde, V. Veryazov, P. O. Widmark, M. Cossi, B. Schimmelpfennig, P. Neogrady and L. Seijo, *Comput. Mater. Sci.,* 2003, **28**, 222.

27. (a) F. Neese, T. Petrenko, D. Ganyushin and G. Olbrich, *Coord. Chem. Rev.*, 2007, **251**, 288; (b) F. Neese, The ORCA program system. Wiley Interdisciplinary Reviews-Computational Molecular Science, 2012, **2**, 73; (c) F. Neese, ORCA; University of Bonn: Bonn, Germany, 2010.

28. L. Banci, A. Bencini, C. Benelli, D. Gatteschi, C. Zanchini, Struct. Bonding, 1982, **52**, 37.

29. (a) A. Arauzo, A. Lazarescu, S. Shova, E. Bartolomé, R. Cases, J. Luzón, J. Bartolomé and C. Turta, *Dalton Trans*., 2014, **45**, 12342; (b) H. X. Zhang, S. Y. Lin, S. F. Xue, C. Wang and J. K. Tang, *Dalton Trans.*, 2015, **44**, 4648.

30. (a) F. Habib, I. Korobkov and M. Murugesu, *Dalton Trans.,* 2015, **44**, 6368; (b) Z. B. Hu, Z. Y. Jing, M. M. Li, L. Yin, Y. D. Gao, F. Yu, T. P. Hu, Z. Wang and Y. Song, *Inorg. Chem.,* 2018, **57**, 10761; (c) J.Li, Y. Han, F. Cao, R. M. Wei, Y. Q. Zhang and Y. Song. *Dalton Trans.,* 2016, **45**, 9279; (d) I. Potoèòák, K. Ráczová, E. Èižmár, L. Váhovská, O. Bukrynov, S.Vitushkina and L. Findoráková, *Polyhedron*, 2017, **137**, 112.

31.- B. Drahoš, R. Herchel and Z. Trávnícek, *Inorg. Chem.* 2017, **56**, 5076. (e) Y. P. Tupolova, I. N. Shcherbakov, L. D. Popov, V. E. Lebedev, V. V. Tkachev, K. V. Zakharov, A. N. Vasiliev, D. V. Korchagin, A. V. Palii and S M. Aldoshin, *Dalton Trans.* 2019, **48**, 6960.

32. A. Abragam and B.Bleaney, Electron Paramagnetic Resonance of Transition Ions, Clarendon Press. Oxford, 1970.

33. (a) A. Singh and K. N. Shrivastava, *Phys. Status Solidi B*, 1979, **95**, 273; (b) K. N. Shirivastava, *Phys. Status Solidi B*, 1983, **117**, 437.

34. A. Lunghi, F. Totti, R. Sessoli and S. Sanvit, *Nature Communications*, 2017, **8**, 14620.

35. A. Lunghi, F. Totti, S. Sanvit and R. Sessoli, *Chem. Sci*., 2017, **8**, 6051.

36. E. Colacio, J. Ruiz, A. Mota, M. A. Palacios, E. Cremades, E. Ruiz, F. J. White and E. K. Brechin, *Inorg. Chem.,* 2012, **51**, 5857.

37. A. K. Hassan, L. A. Pardi, J. Krzystek, A. Sienkiewicz, P. Goy, M. Rohrer and L. C. Brunel, *J. Magn. Reson.,* 2000, **142**, 300.

38. APEX2; Bruker AXS: Madison, WI, 2010.

39. SAINT, Version 8.30a; Bruker AXS: Madison, WI, 2013.

40. Sheldrick, G. M. SADABS, Version 2004/1; Bruker AXS:Madison, WI, 2008.

41. G. M. Sheldrick, SHELXL-97, A Program for Crystal Structure Refinement. University of Göttingen, Germany, 1997. SHELXTL Version 2014/7. http://shelx.uni-ac.gwdg.de/SHELX/index.php.

42. L. F. Chibotaru and L. Ungur, *J. Chem. Phys*., 2012, **137**, 064112.

43. (a) B. O.Roos, V. Veryazov and P. O. Widmark, *Theor. Chim. Acta*., 2004, **111**, 345; (b) B. O. Roos, R. Lindh, P. A. Malmqvist, V. Veryazov and P. O. Widmark, *J. Phys. Chem. A,* 2004, **108**, 2851; (c) B. O. Roos, R. Lindhn, P. A. Malmqvist, V. Veryazov and P. O. Widmark, *J. Phys. Chem. A,* **2005**, **109**, 6575; (d) B. O. Roos, R. Lindh, P. A. Malmqvist, V. Veryazov and P. O. Widmark, *Chem. Phys. Letters,* 2005, **409**, 295.

44. M. Douglas and N. M. Kroll, *Annals of Physics,* 1974**, 82**, 89.

45. (a) F. Weigend and R. Ahlrichs, *Phys. Chem. Chem. Phys.*, 2005, **7**, 3297; (b) A. Schaefer, H. Horn and R. Ahlrichs, *J. Chem. Phys.*, 1992, **97**, 2571; (c) A. Schaefer, C. Huber and R. Ahlrichs, *J. Chem. Phys.*, 1994, **100**, 5829; (d) A. Schäfer, C. Huber and R. Ahlrichs, *The Journal of Chemical Physics* 1994**, 100**, 5829.

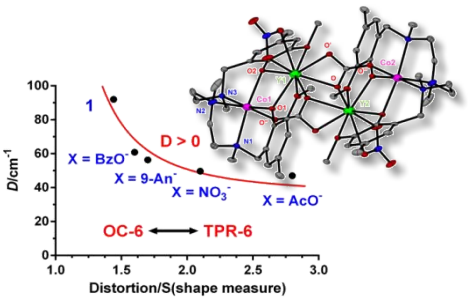

A new $Co^{II}_2Y^{III}_2$ complex has been prepared with aim of comparing its magnetic properties with those of the $Co^{II}Y^{III}$ counteparts. The lower distortion of the Co^{II} ions leads to a large magnetic anisotropy, whereas its larger size and flexibility seems to promote a fast relaxation dynamic.